Molecular Medicine

RESEARCH ARTICLE

Open Access

Soy isoflavones induces mitophagy to inhibit the progression of osteosarcoma by blocking the AKT/mTOR signaling pathway

Ziang Zheng[1†], Xinghan Zhao[1†], Bo Yuan[1], Shan Jiang[1], Rushan Yan[1], Xiaowei Dong[1], Qijun Yao[1] and Haidong Liang[1*]

Abstract

Background Soy isoflavones (SI) is a natural bioactive substance exhibiting beneficial effects on human health. This study aims to elucidate the therapeutic potential of SI in the treatment of osteosarcoma (OS) and to investigate the underlying mechanisms, particularly focusing on mitophagy.

Methods The effects of SI on the proliferation, apoptosis, migration, and invasion of U2OS cells were analyzed. Mitophagy was assessed through multiple parameters: mitochondrial autophagosomes, mitochondrial membrane potential, autophagy-related proteins, reactive oxygen species (ROS), and oxygen consumption rate (OCR). Protein levels related to apoptosis, autophagy, and the AKT/mTOR pathway were analyzed using western blot. The therapeutic efficacy of SI was further identified using a mouse tumor xenograft model. Cell apoptosis and proliferation in tumor xenografts were detected by TUNEL staining and immunohistochemistry (IHC), respectively.

Results SI dose-dependently suppressed the viability, colony formation, migration, and invasion of U2OS cells, and enhanced the apoptosis. SI also dose-dependently induced mitophagy in OS cells, evidenced by an increase in autophagosomes and ROS levels, a decrease in mitochondrial membrane potential and OCR, and concomitant changes in autophagy-related proteins. Mdivi-1, an inhibitor of mitophagy, reversed the anti-tumor effects of SI on U2OS cells. In addition, SI blocked the AKT/mTOR pathway in U2OS cells. SC-79, an AKT agonist, reversed the effect of SI on inducing mitophagy. Moreover, SI also promoted cell apoptosis and mitophagy in tumor xenografts in vivo.

Conclusions SI induces mitophagy in OS cells by blocking the AKT/mTOR pathway, contributing to the inhibition of OS.

Keywords Osteosarcoma, Soy isoflavones, Mitophagy, Autophagy, AKT/mTOR pathway

Background

Osteosarcoma (OS) is a frequent primary bone tumor, characterized by the formation of osteoid or immature bone tissues (Yang et al. 2022). Because OS usually occurs in growing bones, it is more frequent in children and adolescents (Shabani et al. 2019). A second peak in the incidence of OS is observed in individuals around the age of 60 years (Beird et al. 2022). Clinically, surgical intervention coupled with neoadjuvant and postoperative chemotherapy is the standard treatment for

†Ziang Zheng and Xinghan Zhao are co-first authors and contributed equally to this work.

*Correspondence:
Haidong Liang
johnlhddmu@outlook.com
[1] Department of Bone and Soft Tissue Repair and Reconstructive Surgery, The Second Hospital of Dalian Medical University, No. 467 Zhongshan Road, Dalian 116000, Liaoning, China

OS, achieving a five-year survival rate exceeding 70% in patients without metastasis (Lu et al. 2022). However, OS has a strong tendency to metastasis, which poses a great challenge for effective treatment (Chen et al. 2022). The outcomes of metastatic OS remains poor, and the 5-year survival rate is < 20% (Lu et al. 2022). Given the bottleneck encountered in the treatment of OS, particularly for patients with metastasis and chemotherapy resistance, the development of novel drugs with high efficiency and safety is still needed.

Plant-derived bioactive compounds are a series of active substances, which exert multiple pharmacological activities in humans, such as anti-inflammation, antioxidant, anti-stress, antiviral, and anti-tumor (Chen et al. 2022). Soy isoflavones (SI) is an active ingredient found in soybeans and is beneficial for the health of the gastrointestinal tract, heart, and brain, among other systems (Al-Nakkash and Kubinski 2020; Sekikawa et al. 2019). As a phytoestrogen, SI is also closely associated with a low incidence of hormone-related cancers such as breast and prostate cancers (Varinska et al. 2015; Sivonova et al. 2019). A meta-analysis based on 8 articles reported that the consumption of SI is associated with a reduced risk of breast cancer in women before and after menopause (Boutas et al. 2022). Another meta-analysis based on 30 articles revealed that the consumption of SI is positively associated with a low risk of prostate cancer (Applegate et al. 2018). In addition, evidence has also determined that SI can sensitize cancer cells to chemoradiotherapy but not affect normal cells (Sahin et al. 2019). However, the detailed effects of SI in OS and relevant molecular mechanisms are rarely reported yet.

Mitophagy, a specialized form of autophagy targeting mitochondria, plays an essential role in maintaining mitochondrial function (Zhang et al. 2022). Mitophagy exerts a crucial role in tumorigenesis and progression, but its function is still controversial in different types of cancers (Panigrahi et al. 2020). As reported, the activation of mitophagy can promote the progression of breast cancer (Li et al. 2022) and hepatocellular carcinoma (Yao et al. 2022). On the contrary, mitophagy exerts a tumor-suppressor role in glioma (Huang et al. 2021), cervical (Sun et al. 2022), ovarian (Meng et al. 2022), colon (Yin et al. 2021), and lung cancers (Hwang et al. 2022). Previous studies have indicated that various potential therapeutic agents, including protodioscin (Huang et al. 2023), ZnO nanoparticles (He et al. 2020), parthenolide (Yang et al. 2016), and norcantharidin (Mei et al. 2019), can inhibit OS progression by inducing mitophagy. Of note, SI also participates in the regulation of mitophagy. Li M et al. reported that genistein alleviates the senescence of bone marrow mesenchymal stem cells through inducing mitophagy (Li et al. 2023). Li et al. revealed that SI protects neurons from the toxicity of atrazine by inducing mitophagy (Li et al. 2021). However, whether the role of SI in OS is associated with mitophagy is still unclear.

The pathogenesis of cancers is complex and involves a multitude of signaling pathways. The AKT/mTOR signaling pathway is regarded as a promising therapeutic target for human cancers (Yu et al. 2022). Evidence has determined that the AKT/mTOR pathway also participates in the process of mitophagy (Zhao et al. 2022; Zheng et al. 2021; Liu et al. 2021). Of note, Zhang et al. reported that SI alleviates hypoxic damage in neuronal cells by blocking the AKT/mTOR pathway (Zhang et al. 2022). Therefore, mitophagy that is mediated by the AKT/mTOR pathway may be involved in the action mechanisms of SI in OS.

In the current research, we examined the effects of SI on OS using both in vitro and in vivo models. Moreover, the action mechanisms of SI involving mitophagy and the AKT/mTOR pathway were analyzed. By delving deeper into these molecular interactions, this study aims to not only shed light on the multifaceted action of SI in OS treatment but also to explore its potential as a novel, efficacious therapeutic agent, thereby contributing to the advancement of cancer therapy.

Methods

Cell culture and treatments

Human OS cell lines U2OS, Saos2, and MG63 (Pricella, Wuhan, China; Catalog No: CL-0236, CL-0202, and CL-0157, respectively) were cultured in RPMI-1640 medium (HyClone, Logan, UT, USA; Catalog No: 8120348) with 10% fetal bovine serum (FBS; Ephraim, Xiamen, China; Catalog No: 34080619) at 37 °C with 5% CO_2. For treatments, U2OS cells were incubated with SI, which was obtained as an analytical standard with 80% purity from Shanghai Yuanye Bio-Technology Co., Ltd. (Shanghai, China; Catalog No: 574-12-9; 10, 20, and 40 μM) for 48 h. In addition, a part of the U2OS cells were pre-treated with 50 mM Mdivi-1 (an inhibitor of mitophagy; Beyotime, Beijing, China; Catalog No: SC8028-5 mg) for 1 h and then incubated with 40 μM SI for another 48 h. Another part of U2OS cells were incubated with 40 μM SI combined with 5 μM SC-79 (an AKT agonist; Beyotime; Catalog No: SF2730-5 mg) for 48 h or pre-treated with 10 nM MK-2206 (an AKT inhibitor; Beyotime; Catalog No: SF2712-10 mM) for 1 h and then incubated with 40 μM SI for another 48 h.

Cell Counting Kit-8 (CCK-8) assay

Cell viability was assessed using a CCK-8 kit (Beyotime; Catalog No: C0037). Briefly, 100 μL U2OS cells that were seeded in 96-well plates were incubated with SI for 12, 24, 48, and 96 h, respectively. After 2 h of incubation with 10 μL CCK-8, optical density at 450 nm was measured in

each well by a microplate reader (DR-3518G, Hiwell Diatek, Wuxi, China).

Colony-formation assay

Colony-formation assay was performed to reflect the state of cell proliferation. In brief, U2OS cells were seeded into 6-well plates in an initial quantity of 200 cells/well. After 14 days of culturing, the former colonies were stained with crystal violet (Beyotime; Catalog No: C0121-100 mL) for 20 min and counted in each well.

Wound-healing assay

Wound-healing assay was performed to evaluate cell migration. In brief, U2OS cells were cultured overnight in 6-well plates. A wound track was made in each well along the diameter. After 24 h of continuous culturing, the width of the wound gap was quantified. The migration rate was calculated as (distance$^{0\ h}$- distance$^{24\ h}$)/distance$^{0\ h}\times 100\%$.

Trans-well assay

Trans-well assay was performed to evaluate cell invasion. Briefly, a matrigel-coated upper chamber was added with 200 μL U2OS cells, and the lower chamber was added with RPMI 1640 medium containing 20% FBS. After 24 h, cells in the lower chamber were collected and then stained with crystal violet for 20 min. Invasive cells, stained violet, were quantified under a microscope (CKX53, Olympus, Japan).

Transmission electron microscopy (TEM)

Mitochondrial autophagosomes were observed by TEM. In brief, U2OS cells were fixed in 2.5% glutaraldehyde (Sinopharm, Shanghai, China; Catalog No: 30092436), dehydrated in alcohol (Sinopharm; Catalog No: 10009218) and acetone (Sinopharm; Catalog No: 10000418), embedded in epoxy resin (Solarbio, Beijing, China; Catalog No: G8590), and sliced. After stained with 2% sodium acetate-lead citrate (Sinopharm; Catalog No: 6131-90-4 and Macklin, Shanghai, China; Catalog No: 512-26-5, respectively), the samples were captured under a TEM microscope (JEM-1400FLASH, JEOL, Japan).

Immunofluorescence (IF)

The location and expression of LC3 in U2OS cells were detected by IF. Briefly, U2OS cells that were seeded in 12-well plates were stained with Mito-Tracker Green solution (Beyotime; Catalog No: C1048) for 30 min. After being washed with phosphate-buffered saline (Beyotime; Catalog No: C0221A), cells were fixed in 3% methanol (Sinopharm; Catalog No: 80080418), treated with 1% Triton-X 100 (Solarbio, Catalog No: T8200), and blocked with 3% bovine serum albumin (Sigma-Aldrich, St Louis, MO, USA; Catalog No: A7906). Subsequently, cells underwent 12 h of incubation with anti-LC3 (1:250, Abcam, Cambridge, UK; Catalog No: ab192890) at 4 °C, and further underwent 1 h of incubation with Alexa Fluor® 647-IgG (1: 500, Abcam; Catalog No: ab150079) and 4′, 6-diamidino-2-phenylindole (DAPI) (Beyotime; Catalog No: C1005) at 25 ℃. After quenching and sealing, cells displaying fluorescence were observed under a microscope (CKX53, Olympus).

Flow cytometry

Using an Apoptosis Detection Kit (Beyotime; Catalog No: C1062S), sample cells were labeled with 5 μL Annexin V-FITC and 10 μL propidium iodide to detect apoptosis. Using a Mitochondrial Membrane Potential Detection Kit (Beyotime; Catalog No: C2006), sample cells were labeled with JC-1 to detect mitochondrial membrane potential. Using ROS Detection Kit (Beyotime; Catalog No: S0033S), sample cells were labeled with DCFH-DA fluorescence probe to detect ROS level. Data acquired from the flow cytometer (CytoFLEX S, Beckman, Miami, FL, USA) were analyzed using Cell Quest software (BD Biosciences, Franklin Lake, NJ, USA).

Oxygen consumption rate (OCR) assay

OCR was detected by an extracellular flux analyzer (XFe96, Agilent, Santa Clara, CA, USA). In brief, U2OS cells that were seeded in XF96e plates were cultured overnight at 37 °C. Subsequently, cells were incubated for 70 min in a CO_2-free assay medium. During culturing, oligomycin (3 μM; Sigma-Aldrich; Catalog No: 75351), FCCP (0.5 μM; Sigma-Aldrich, Catalog No: C2920), and rotenone combined with antimycin A (both 1 μM; Sigma-Aldrich, Catalog No: R8875 and A8674, respectively) were added at the 20th, 35th, and 50th min, respectively.

Establishment of tumor xenograft model in mice

BALB/c nude mice (male, 4 weeks old) were obtained from HFK Bioscience (Beijing, China). After a one-week acclimatization period, 100 μL U2OS cells (2×10^6 cells/mL) were subcutaneously injected into the right flank to induce the xenograft OS model. For the construction of a lung metastatic model, 4-week-old male BALB/c nude mice were injected with 100 μL U2OS cells (2×10^6 cells/mL) via the tail vein. After the tumor reached 100 mm^3, 40 mg/kg SI was gavaged in mice once a day (N = 5). Mice in the control group were gavaged with an equal volume of physiological saline (N = 5). Via measuring tumor diameter every 4 days, the tumor volume was calculated as: $0.5\times(\text{diameter}_{\text{longest}}\times\text{diameter}_{\text{shortest}}^{2})$. Twenty-eight days later, mice were anesthetized with 50 mg/kg pentobarbital sodium and then sacrificed by cervical dislocation. The tumor xenografts were resected, photographed,

and weighted. All animal experimental procedures were sanctioned by the Ethics Committee of Yangzhou University School of Medicine and were conducted following the Guide for the Care and Use of Laboratory Animals (202303137).

TUNEL staining and immunohistochemistry (IHC)

TUNEL staining and IHC were performed to detect the apoptosis and proliferation of tumor cells in vivo, respectively. In brief, the xenograft samples were fixed in 4% paraformaldehyde (Sinopharm; Catalog No: 10010018), dehydrated in graded ethanol, vitrificated in xylene (Sinopharm; Catalog No: 10023418), embedded in paraffin, and sliced at 5–7 μm. For TUNEL staining, the sliced samples were stained with TUNEL (Beyotime; Catalog No: C1086) for 60 min and then with DAPI for another 10 min under darkness. For IHC, the sliced samples were incubated with anti-Ki67 (1:200, Abcam; Catalog No: ab15580) for 12 h, and then with horseradish peroxidase (HRP)-conjugated IgG (1:500, Abcam; Catalog No: ab205718) for another 1 h. After incubation with diaminobenzidine (Beyotime; Catalog No: p0203) for 30 min under darkness, the samples were re-stained with hematoxylin for another 3 min. After quenching and sealing, the stained sections were observed under a microscope (CKX53, Olympus).

Hematoxylin and eosin (HE) staining

Lung tissue samples were fixed in 4% paraformaldehyde for 24 h, embedded in paraffin wax, and cut into 4–7 μm sections. The sections were immersed in xylene for 15 min, followed by rehydration through a graded alcohol series. Then, sections were stained with hematoxylin solution for 5 min and eosin solution for 1 min. After being mounted with a resinous, the sections were observed under a microscope to assess the histological features.

Western blot

Total proteins in U2OS cells or tumor xenografts were extracted by lysing in RIPA buffer (Beyotime; Catalog No: P0013B). Equal amounts of protein from different groups were separated via 8% sodium dodecyl sulfate–polyacrylamide gel electrophoresis and transferred to polyvinylidene fluoride membranes. Subsequently, the membranes carrying protein samples were blocked with blocking buffer (Beyotime; Catalog No: P0216-300 g) for 1 h, incubated with specific primary antibody for 12 h, and further incubated with specific secondary antibody (HRP-conjugated IgG, 1:2000, Abcam) for 1 h under darkness. After visualizing using a hypersensitive chemiluminescence kit (Beyotime; Catalog No: P0018S), the blots were analyzed by a Gel Imaging System (3500, Tanon, China). The primary anti-bodies used in western blot included anti-Bax (1:5000, Abcam; Catalog No: ab32503), -Bcl-2 (1:1000, Abcam; Catalog No: ab32124), -pro caspase-3 (1:1000, Abcam; Catalog No: ab32150), -cleaved caspase-3 (1:5000, Abcam; Catalog No: ab214430), -P62 (1:1000, Abcam; Catalog No: ab207305), -LC3 (1:2000, Abcam; Catalog No: ab192890), -PINK1 (1:1000, Abcam; Catalog No: ab216144), -Parkin (1:1000, Cell Signaling Technology, Danvers, MA, USA; Catalog No: 2132S), -AKT (1:5000, Abcam; Catalog No: ab227385), -p-AKT (phospho T308; 1:5000, Abcam; Catalog No: ab38449), -mTOR (1:5000, Abcam; Catalog No: ab134903), p-mTOR (phospho S2448; 1:5000, Abcam; Catalog No: ab109268), and -GAPDH (1:5000, Abcam; Catalog No: ab181602).

Statistical analysis

Measurement data were expressed as mean ± standard deviation and were statistically analyzed by GraphPad Prism 7.0 (San Diego, CA, USA). Two-group comparisons were made using an independent t-test, while multiple-group comparisons were made using one-way ANOVA followed by Tukey's post hoc test. A P value < 0.05 represented a statistically significant.

Results

SI suppresses the malignant features of OS cells

Initially, the therapeutic potentials of SI (10, 20, and 40 μM) were assessed against a panel of OS cell lines, namely U2OS, Saos2, and MG63. Notably, U2OS cells exhibited heightened sensitivity to SI, showcasing superior inhibition in cell viability as compared to Saos2 and MG63 cells ($P < 0.05$, Fig. 1A). Consequently, U2OS was selected as the cell line of choice for all subsequent experimental investigations. The viability and colony number of U2OS cells were significantly reduced in a dose-dependent manner following SI treatment ($P < 0.05$,

(See figure on next page.)

Fig. 1 SI inhibits the malignant characteristics of OS cells. **A**, **B** Cell viability was measured by CCK-8 assay; **C** colony number was measured by colony formation assay; **D** cell apoptosis was measured by flow cytometry; **E** the protein expression of Bax, Bcl-2, Pro caspase-3, and Cleaved caspases-3 were measured by Western blot; **F** cell migration was measured by wound-healing assay; G, Cell invasion was measured by trans-well assay. Human OS cell lines U2OS, Saos2, and MG63 were treated with 10 μM, 20 μM, or 40 μM SI for 48 h. All experiments were repeated three times; statistical analysis was performed using one-way ANOVA followed by Tukey's post hoc test. $^{*}P < 0.05$, $^{**}P < 0.01$

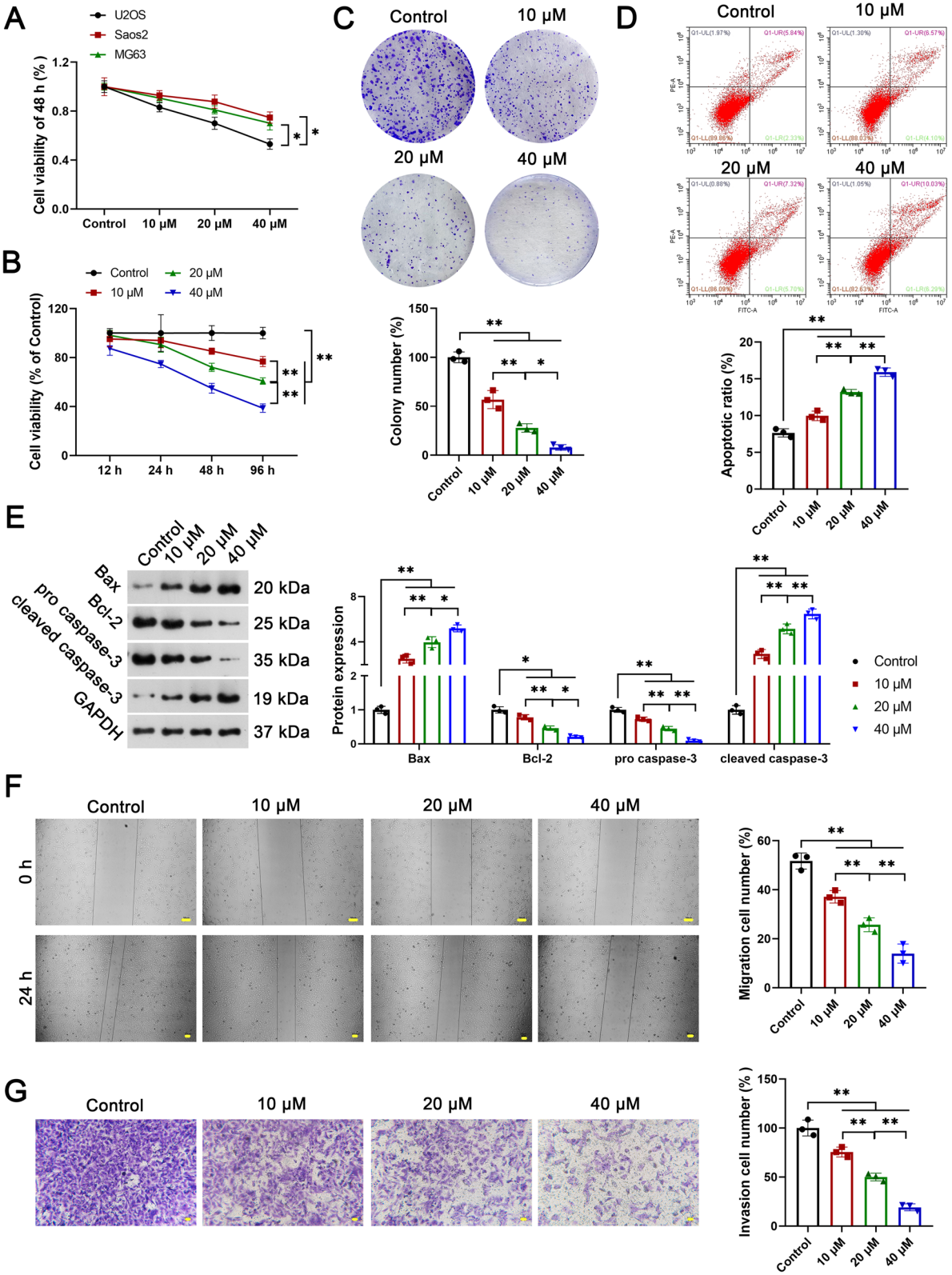

Fig. 1 (See legend on previous page.)

Fig. 1B and C). SI also enhanced the apoptosis of U2OS cells in a dose-dependent manner, as evidenced by a decrease in the apoptotic ratio ($P < 0.01$, Fig. 1D), up-regulation of Bax and Cleaved caspases-3, and down-regulation of Bcl-2 and Pro-caspase-3 ($P < 0.05$, Fig. 1E). Furthermore, significantly fewer cells for migration and invasion were observed in the SI group compared with the control group ($P < 0.01$). Cell migration and invasion were similarly attenuated with increasing concentrations of SI in U2OS cells ($P < 0.01$, Fig. 1F and G).

SI induces mitophagy in OS cells

The effects of SI on mitophagy were subsequently explored in U2OS cells. Under TEM, a higher number of mitochondrial autophagosomes were observed in SI-treated U2OS cells than in the controls, and the number of autophagosomes increased with increasing concentrations of SI (Fig. 2A). Under a fluorescence microscope, LC3 protein that co-located with mitochondria was dose-dependently up-regulated by the intervention of SI (Fig. 2B). SI also dose-dependently down-regulated P62, but up-regulated LC3 II/I, PINK1, and parkin (autophagy-related proteins) in U2OS cells ($P < 0.05$, Fig. 2C). Additionally, the mitochondrial membrane potential was weakened in a dose-dependent manner following SI treatment, as evidenced by a significant decrease in JC-1 red/green ($P < 0.05$, Fig. 2D). The OCR was similarly decreased in a dose-dependent manner following SI treatment ($P < 0.05$, Fig. 2E). Moreover, a dose-dependent increase in ROS was observed in SI-treated U2OS cells compared to the controls ($P < 0.05$, Fig. 2F).

The anti-tumor potential of SI in OS is related to mitophagy activation

To reveal the anti-tumor mechanisms of SI about mitophagy activation, Mdivi-1, an inhibitor of mitophagy, was used for intervention in U2OS cells. As shown in Fig. 3A–D, Mdivi-1 enhanced the viability, migration, and invasion, and reduced the apoptosis of U2OS cells to significant levels ($P < 0.01$). Mdivi-1 also significantly inhibited the mitophagy of U2OS cells, as evidenced by the down-regulation of P62, and up-regulation of LC3 II/I, PINK1, and parkin ($P < 0.01$, Fig. 3E and F). Importantly, Mdivi-1 reversed the effects of SI on inhibiting malignant features and inducing mitophagy in U2OS cells ($P < 0.01$, Fig. 3A–F). Moreover, SI-induced elevation of ROS levels in U2OS cells was weakened by Mdivi-1 intervention ($P < 0.01$, Fig. 3G).

The role of SI in inducing mitophagy is related to the inhibition of the AKT/mTOR pathway

The action mechanisms of SI implicating the AKT/mTOR signaling pathway were subsequently explored. As presented in Fig. 4A, SI at 20 and 40 μM significantly down-regulated p-AKT/AKT and p-mTOR/mTOR in U2OS cells ($P < 0.01$). The effect of SI at 40 μM was stronger than that at 20 μM in inhibiting the AKT/mTOR pathway ($P < 0.01$). Subsequently, the AKT/mTOR pathway was actively activated using SC-79 (AKT agonist) or blocked using MK-2206 (AKT inhibitor) in U2OS cells ($P < 0.01$, Fig. 4B). SC-79 reversed the effects of SI on down-regulating P62, and on up-regulating LC3 II/I, PINK1, and parkin ($P < 0.05$). In contrast, MK-2206 aggravated the effects of SI on inducing mitophagy ($P < 0.01$, Fig. 4C and D).

SI inhibits the growth and metastasis of OS xenografts in vivo

The effects of SI in OS were further verified in a xenograft mouse model. As presented in Fig. 5A–C, the gavage of SI inhibits the growth of tumor xenografts in mice, as evidenced by the significant decrease in tumor weight on the 28th day and in tumor volume beginning from the 16th day ($P < 0.01$). In addition, more apoptotic cells positive for TUNEL and less active cells positive for Ki67 were observed in SI-treated mice compared with the controls (Fig. 5D and E). HE staining revealed obvious cellular infiltration in the lung tissues (Fig. 5F). However, SI significantly inhibited the metastasis of OS toward the lung ($P < 0.01$, Fig. 5F). Moreover, western blot revealed that the gavage of SI significantly down-regulated P62, and up-regulated LC3 II/I, PINK1, and parkin in tumor xenografts ($P < 0.01$, Fig. 5G).

Discussion

OS is a prevalent bone malignancy characterized by a high mortality rate, primarily due to its strong tendency for pulmonary metastasis (Cui et al. 2020). Despite advancements in therapeutic regimens, the clinical

(See figure on next page.)

Fig. 2 SI induces mitophagy in OS cells. **A** Mitochondrial autophagosomes were observed under TEM; **B** the location and expression of LC3 were detected by IF; **C** the protein expression of P62, LC3 II/I, PINK1, and parkin (autophagy-related proteins) were detected by western blot; **D** the mitochondrial membrane potential (JC-1 red/green) was detected by flow cytometry; **E** the OCR was measured by an extracellular flux analyzer; **F** the ROS was measured by flow cytometry. Human OS cell lines U2OS, Saos2, and MG63 were treated with 10 μM, 20 μM, or 40 μM SI for 48 h. All experiments were repeated three times; statistical analysis was performed using one-way ANOVA followed by Tukey's post hoc test. $^{*}P < 0.05$, $^{**}P < 0.01$

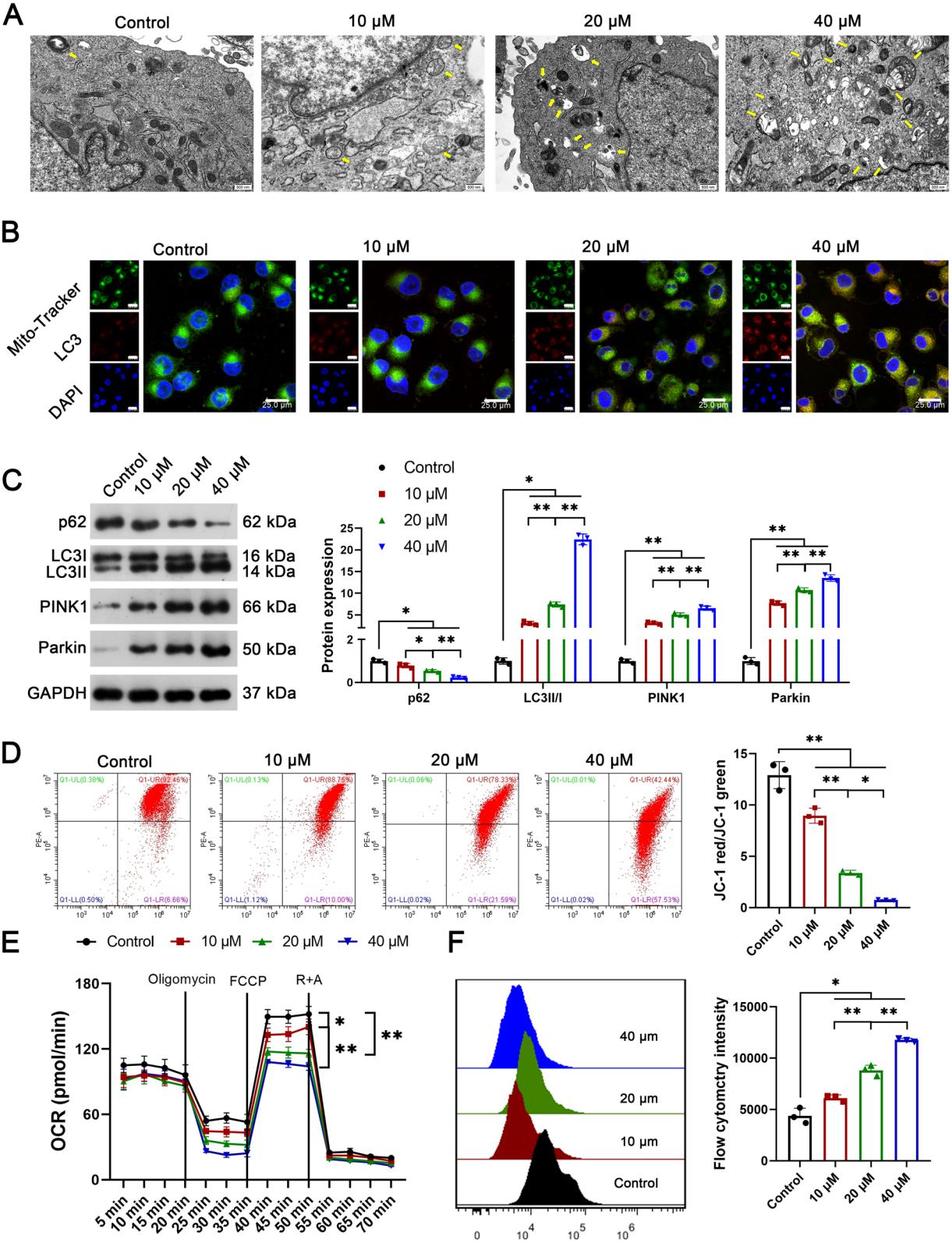

Fig. 2 (See legend on previous page.)

outcomes for patients with OS remain unsatisfactory. In the present study, the anti-tumor effects and mechanisms of SI on OS were explored. Our study revealed that SI suppressed the malignant characteristics of OS cells in vitro, as well as the growth of OS xenografts in vivo. The activation of mitophagy, mediated by the AKT/mTOR pathway, is involved in the action mechanisms of SI in OS.

Plant-derived bioactive compounds are active substances that received much attention in clinical use. More and more studies have revealed that plant-derived bioactive compounds exhibit promising therapeutic potential against tumors, such as glycosides, flavonoids, polyphenols, polysaccharides, phenols, quercetin, etc. (Esmeeta et al. 2022; Raju et al. 2022). SI belongs to the class of phytoestrogens and possesses a structural similarity to the human 17-beta estradiol hormone (Boutas et al. 2022). SI exerts beneficial effects on lowering blood lipids and glucose, inhibiting oxidative stress, preventing osteoporosis, and reducing the risk of breast and prostate cancer (Varinska et al. 2015; Sivonova et al. 2019; Nakai et al. 2020). Genistein and daidzein are two major active constituents of SI, exhibiting significant biological functions in humans (Song et al. 2015). By affecting cell apoptosis, cell cycle, metastasis, and angiogenesis, genistein exhibits great therapeutic potential against diverse types of cancers (Spagnuolo et al. 2015). Similarly, daidzein also exerts anti-tumor activity against lung cancer (Guo et al. 2020), breast cancer (Alshehri et al. 2021), bladder cancer (He et al. 2016), ovarian cancer (Hua et al. 2018), etc. Of note, Song et al. demonstrated that genistein suppresses the viability and enhances the apoptosis of OS cells (Song et al. 2015). Zhu et al. revealed that daidzein suppresses the proliferation and migration of OS cells (Zhu et al. 2021). Here, the effects of SI on the malignant features of OS were explored. As a result, SI dose-dependently suppressed the proliferation, migration, and invasion, and enhanced the apoptosis of U2OS cells. These results are similar to previous studies on genistein and daidzein mentioned above and demonstrate a positive role of SI in inhibiting OS cells in vitro. Furthermore, our in vivo experiments corroborated these findings, demonstrating that SI not only reduced tumor volume and weight but also increased the proportion of apoptotic cells while decreasing the number of active cells in OS xenografts. Our findings confirmed a promising efficiency of SI in the treatment of OS.

Mitophagy is a conserved intracellular process that is important for mitochondrial health. Via removing dysfunctional or superfluous mitochondria in cells, mitophagy plays a crucial role in various human diseases, including cardiovascular, neurodegenerative, and metabolic diseases, and cancers (Lu et al. 2023). In this study, the mitophagy was activated in OS cells by the intervention of SI, evidenced by the increase in autophagosomes and ROS, a decrease in mitochondrial membrane potential and OCR, and changes in autophagy-related proteins. As previously reported, the activation of mitophagy contributes to the treatment of cervical cancer (Sun et al. 2022), colon cancer (Yin et al. 2021), glioma (Huang et al. 2021), ovarian cancer (Meng et al. 2022), lung cancer (Hwang et al. 2022), etc. The anti-tumor role of some agents in OS is also related to the activation of mitophagy. For example, protodioscin inhibits the viability and enhances the apoptosis and mitophagy of OS cells (Huang et al. xxxx). The effects of norcantharidin on inhibiting cell proliferation, migration, and invasion are related to mitophagy in OS (Mei et al. 2019). Parthenolide activates mitophagy-mediated cell death in OS (Yang et al. 2016). Based on these findings, our findings suggest that the activation of mitophagy may participate in the anti-tumor mechanisms of SI in OS. To further verify this regulatory mechanism, mitophagy was actively inhibited using Mdivi-1 in subsequent experiments. Encouragingly, mdivi-1 reversed the effects of SI on inhibiting the malignant characteristics of U2OS cells. Therefore, SI may inhibit the progression of OS by inducing mitophagy.

Many signaling pathways participate in the initiation and progression of OS, such as the Wnt/β-catenin, AKT/mTOR, Notch, HIF-1α, P53, MAPK, and JNK pathways (Han and Shen 2020). Among them, the AKT/mTOR pathway is a well-known regulator in multiple cellular functions (Alzahrani 2019). In this study, the AKT/mTOR pathway was significantly inhibited in OS cells following SI treatment, a finding that is consistent with a previous study demonstrating that SI alleviates hypoxic damage in neuronal cells via blocking the

(See figure on next page.)

Fig. 3 Inhibition of mitophagy reversed the anti-tumor effects of SI on OS cells. **A** Cell viability was measured by CCK-8 assay; **B** cell apoptosis was measured by flow cytometry; **C** cell migration was measured by wound-healing assay; **D** cell invasion was measured by trans-well assay; **E** the location and expression of LC3 were detected by IF; **F** the protein expression of P62, LC3 II/I, PINK1, and parkin (autophagy-related proteins) were detected by western blot; **G** The ROS was measured by flow cytometry. U2OS cells were pre-treated with 50 mM autophagy inhibitor Mdivi-1 for 1 h and then treated with 40 μM SI for 48 h. All experiments were repeated three times; statistical analysis was performed using one-way ANOVA followed by Tukey's post hoc test. $^{*}P < 0.05$, $^{**}P < 0.01$

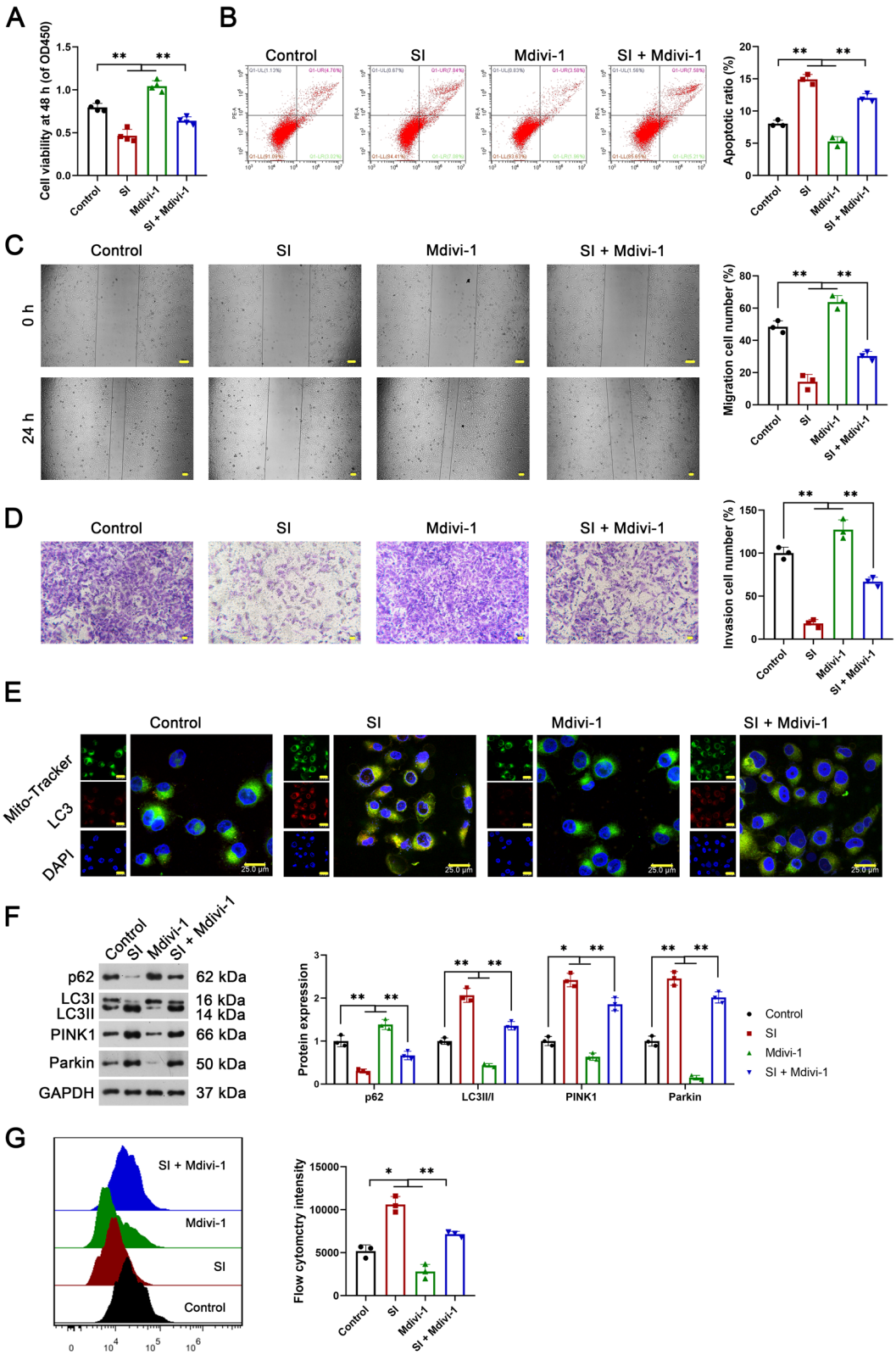

Fig. 3 (See legend on previous page.)

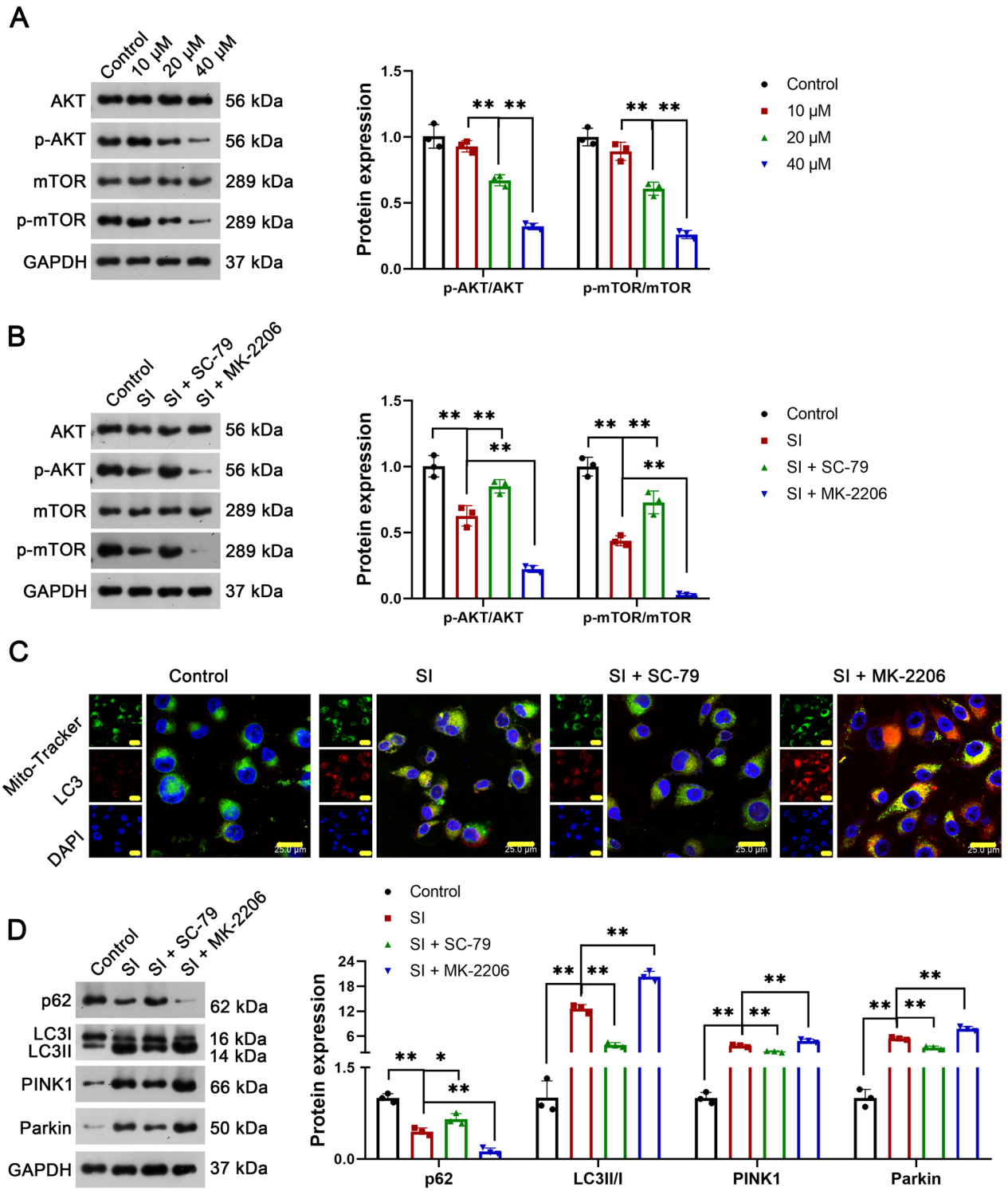

Fig. 4 The activation of the AKT/mTOR pathway reversed the effects of SI on inducing mitophagy in OS cells. **A** The protein expression of p-AKT/AKT and p-mTOR/mTOR in U2OS cells treated with SI were detected by western blot; U2OS cells were treated with 10 μM, 20 μM, or 40 μM SI for 48 h. **B** The protein expression of p-AKT/AKT and p-mTOR/mTOR in U2OS cells treated with SI combined with SC-79 (AKT agonist) or MK-2206 (AKT inhibitor) were detected by western blot; **C** the location and expression of LC3 were detected by IF; **D** the protein expression of P62, LC3 II/I, PINK1, and parkin (autophagy-related proteins) were detected by western blot. U2OS cells were co-treated with 40 μM SI and 5 μM SC-79 (AKT agonist) or 10 nM MK-2206 (AKT inhibitor) for 48 h. All experiments were repeated three times; statistical analysis was performed using one-way ANOVA followed by Tukey's post hoc test. $^{*}P < 0.05$, $^{**}P < 0.01$

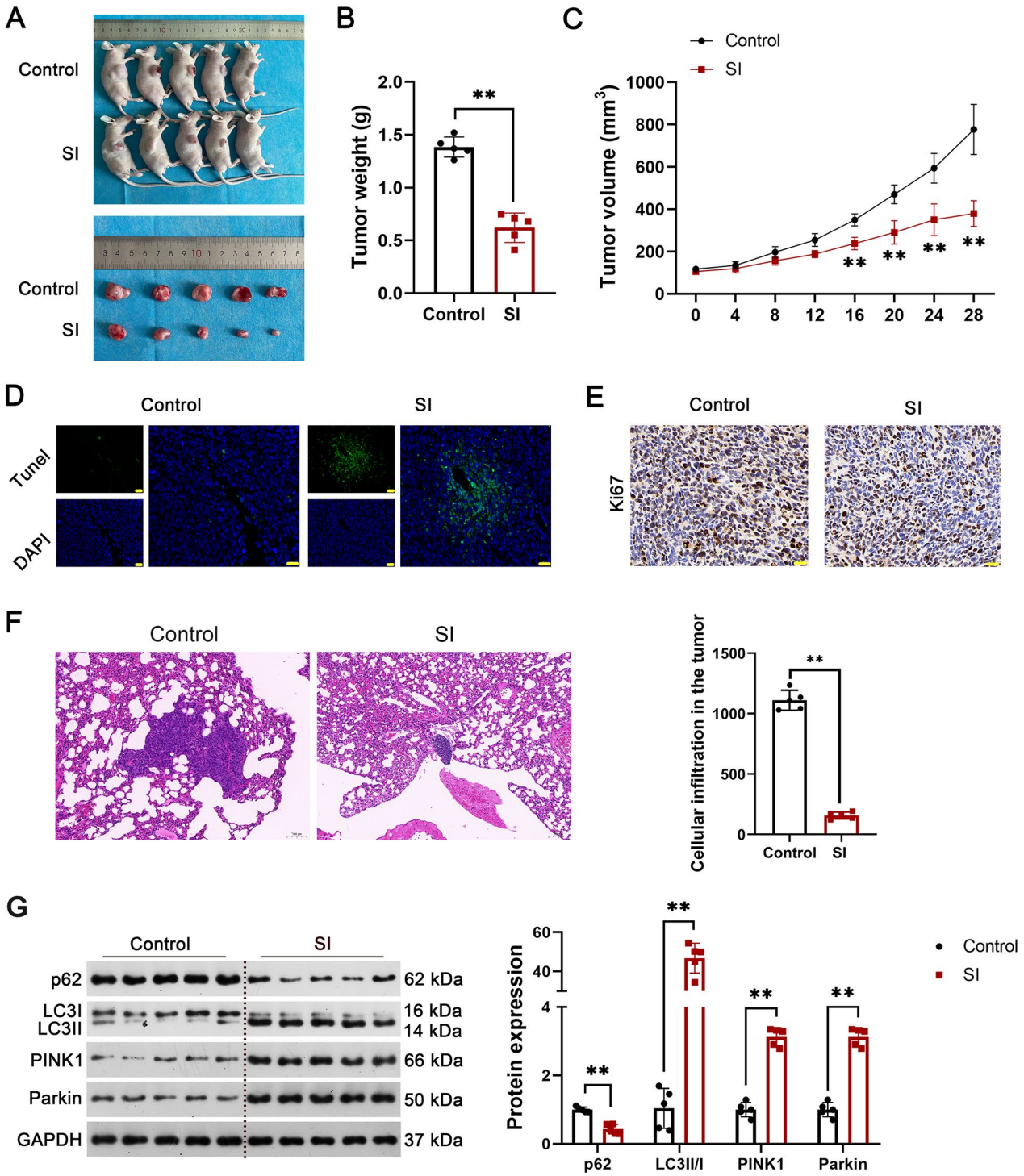

Fig. 5 SI inhibits the growth of tumor xenografts in mice. **A** The morphology of the mouse model and separated tumor xenografts; **B** the tumor weight on the 28th day; **C** the tumor volumes every 4 days; **D** the apoptotic cells were detected by TUNEL staining; **E** the active cells were detected by IHC of Ki67; **F** HE staining for lung tissues; **G** the protein expression of P62, LC3 II/I, PINK1, and parkin (autophagy-related proteins) were detected by western blot. OS model mice were gavaged with 40 mg/kg SI once a day for 28 days. Experiments were performed with five mice per group; statistical analysis was performed using an independent t-test. $^{**}P < 0.01$

AKT/mTOR pathway (Zhang et al. 2022). In addition, the AKT/mTOR pathway also plays a key regulatory role in mitophagy. Zhao et al. reported that leonurine activates mitophagy to protect against oxidative stress-induced damage in bone mesenchymal stem cells by blocking the PI3K/Akt/mTOR pathway (Zhao et al. 2022). Zheng et al. revealed that rapamycin inhibits apoptosis and enhances the mitophagy of neuronal cells by blocking the PI3K/AKT/mTOR pathway (Zheng et al. 2021). Liu et al. demonstrated that Zhen-Wu-Tang activates mitophagy to relieve renal mitochondrial dysfunction via inhibiting the PI3K/AKT/mTOR pathway (Liu et al. 2021). Combined with the positive effects of SI on inducing mitophagy, we suspect that SI may induce the mitophagy of OS cells by blocking the AKT/mTOR pathway. Encouragingly, our following experiments verified this speculation, as evidenced by that the activation of the AKT/mTOR pathway reversed the effects of SI on inducing mitophagy.

Conclusions

In conclusion, our findings demonstrate that SI exerts anti-tumor effects in OS both in vitro and in vivo, positioning it as a potentially promising therapeutic agent. The therapeutic potential of SI in OS appears to be intricately linked with the activation of mitophagy, which is mediated via the AKT/mTOR signaling pathway.

Abbreviations

SI	Soy isoflavones
OCR	Oxygen consumption rate
IHC	Immunohistochemistry
OS	Osteosarcoma
CCK-8	Cell Counting Kit-8
TEM	Transmission electron microscopy
IF	Immunofluorescence
HRP	Horseradish peroxidase

Acknowledgements

Not applicable.

Author contributions

ZZ and XZ substantially contributed to the conception and the design of the study. ZZ, XZ and SJ were responsible for the acquisition, analysis and interpretation of the data. RY and BY confirm the authenticity of all the raw data. XD, QY and HL contributed to manuscript drafting and critical revisions of the intellectual content. BY and HL approved the final manuscript to be published and obtained the funding. ZZ and XZ are contributed equally. All authors read and approved the final manuscript.

Funding

This work was supported by [The cultivating scientific research project of the Second Hospital of Dalian Medical University] [Number dy2yynpy202219].

Availability of data and materials

The datasets used and analysed during the current study are available from the corresponding author on reasonable request.

Declarations

Ethics approval and consent to participate

All animal experimental procedures were sanctioned by the Ethics Committee of Yangzhou University School of Medicine and were conducted following the Guide for the Care and Use of Laboratory Animals (202303137).

Consent for publication

All authors have given their consent for the publication of the final version.

Competing interests

The authors declare that they have no competing interests.

Received: 8 August 2023 Accepted: 2 January 2024
Published online: 08 January 2024

References

Al-Nakkash L, Kubinski A. Soy isoflavones and gastrointestinal health. Curr Nutr Rep. 2020;9(3):193–201.
Alshehri MM, Sharifi-Rad J, Herrera-Bravo J, Jara EL, Salazar LA, Kregiel D, et al. Therapeutic potential of isoflavones with an emphasis on daidzein. Oxid Med Cell Longev. 2021;2021:6331630.
Alzahrani AS. PI3K/Akt/mTOR inhibitors in cancer: at the bench and bedside. Semin Cancer Biol. 2019;59:125–32.
Applegate CC, Rowles JL, Ranard KM, Jeon S, Erdman JW. Soy consumption and the risk of prostate cancer: an updated systematic review and meta-analysis. Nutrients. 2018;10(1):40.
Beird HC, Bielack SS, Flanagan AM, Gill J, Heymann D, Janeway KA, et al. Osteosarcoma. Nat Rev Dis Primers. 2022;8(1):77.
Boutas I, Kontogeorgi A, Dimitrakakis C, Kalantaridou SN. Soy isoflavones and breast cancer risk: a meta-analysis. In Vivo. 2022;36(2):556–62.
Chen X, Pan S, Li F, Xu X, Xing H. Plant-derived bioactive compounds and potential health benefits: involvement of the gut microbiota and its metabolic activity. Biomolecules. 2022;12(12):1871.
Cui J, Dean D, Hornicek FJ, Chen Z, Duan Z. The role of extracelluar matrix in osteosarcoma progression and metastasis. J Exp Clin Cancer Res. 2020;39(1):178.
Esmeeta A, Adhikary S, Dharshnaa V, Swarnamughi P, Ummul Maqsummiya Z, Banerjee A, et al. Plant-derived bioactive compounds in colon cancer treatment: an updated review. Biomed Pharmacother. 2022;153: 113384.
Guo S, Wang Y, Li Y, Feng C, Li Z. Daidzein-rich isoflavones aglycone inhibits lung cancer growth through inhibition of NF-kappaB signaling pathway. Immunol Lett. 2020;222:67–72.
Han J, Shen X. Long noncoding RNAs in osteosarcoma via various signaling pathways. J Clin Lab Anal. 2020;34(6): e23317.
He Y, Wu X, Cao Y, Hou Y, Chen H, Wu L, et al. Daidzein exerts anti-tumor activity against bladder cancer cells via inhibition of FGFR3 pathway. Neoplasma. 2016;63(4):523–31.
He G, Pan X, Liu X, Zhu Y, Ma Y, Du C, et al. HIF-1alpha-mediated mitophagy determines ZnO nanoparticle-induced human osteosarcoma cell death both in vitro and in vivo. ACS Appl Mater Interfaces. 2020;12(43):48296–309.
Hua F, Li CH, Chen XG, Liu XP. Daidzein exerts anticancer activity towards SKOV3 human ovarian cancer cells by inducing apoptosis and cell cycle arrest, and inhibiting the Raf/MEK/ERK cascade. Int J Mol Med. 2018;41(6):3485–92.
Huang T, Xu T, Wang Y, Zhou Y, Yu D, Wang Z, et al. Cannabidiol inhibits human glioma by induction of lethal mitophagy through activating TRPV4. Autophagy. 2021;17(11):3592–606.
Huang CF, Hsieh YH, Yang SF, Kuo CH, Wang PH, Liu CJ, et al. Mitophagy effects of protodioscin on human osteosarcoma cells by inhibition of p38MAPK targeting NIX/LC3 axis. Cells. 2023;12(3):395.
Hwang SK, Jeong YJ, Cho HJ, Park YY, Song KH, Chang YC. Rg3-enriched red ginseng extract promotes lung cancer cell apoptosis and mitophagy by ROS production. J Ginseng Res. 2022;46(1):138–46.
Li P, Yao LY, Jiang YJ, Wang DD, Wang T, Wu YP, et al. Soybean isoflavones protect SH-SY5Y neurons from atrazine-induced toxicity by activating

mitophagy through stimulation of the BEX2/BNIP3/NIX pathway. Ecotoxicol Environ Saf. 2021;227: 112886.
Li Q, Chu Y, Li S, Yu L, Deng H, Liao C, et al. The oncoprotein MUC1 facilitates breast cancer progression by promoting Pink1-dependent mitophagy via ATAD3A destabilization. Cell Death Dis. 2022;13(10):899.
Li M, Yu Y, Xue K, Li J, Son G, Wang J, et al. Genistein mitigates senescence of bone marrow mesenchymal stem cells via ERRalpha-mediated mitochondrial biogenesis and mitophagy in ovariectomized rats. Redox Biol. 2023;61: 102649.
Liu B, Cao Y, Wang D, Zhou Y, Zhang P, Wu J, et al. Zhen-Wu-Tang induced mitophagy to protect mitochondrial function in chronic glomerulonephritis via PI3K/AKT/mTOR and AMPK pathways. Front Pharmacol. 2021;12: 777670.
Lu Y, Zhang J, Chen Y, Kang Y, Liao Z, He Y, et al. Novel Immunotherapies for osteosarcoma. Front Oncol. 2022;12: 830546.
Lu Y, Li Z, Zhang S, Zhang T, Liu Y, Zhang L. Cellular mitophagy: mechanism, roles in diseases and small molecule pharmacological regulation. Theranostics. 2023;13(2):736–66.
Mei L, Sang W, Cui K, Zhang Y, Chen F, Li X. Norcantharidin inhibits proliferation and promotes apoptosis via c-Met/Akt/mTOR pathway in human osteosarcoma cells. Cancer Sci. 2019;110(2):582–95.
Meng Y, Qiu L, Zeng X, Hu X, Zhang Y, Wan X, et al. Targeting CRL4 suppresses chemoresistant ovarian cancer growth by inducing mitophagy. Signal Transduct Target Ther. 2022;7(1):388.
Nakai S, Fujita M, Kamei Y. Health promotion effects of soy isoflavones. J Nutr Sci Vitaminol (tokyo). 2020;66(6):502–7.
Panigrahi DP, Praharaj PP, Bhol CS, Mahapatra KK, Patra S, Behera BP, et al. The emerging, multifaceted role of mitophagy in cancer and cancer therapeutics. Semin Cancer Biol. 2020;66:45–58.
Raju SK, Sekar P, Kumar SV, Murugesan M, Karthikeyan M, Elampulakkadu A. Plant secondary metabolites for the prevention and treatment of colorectal cancer: a review. J Pharmacogn Phytochem. 2022;11:229.
Sahin I, Bilir B, Ali S, Sahin K, Kucuk O. Soy isoflavones in integrative oncology: increased efficacy and decreased toxicity of cancer therapy. Integr Cancer Ther. 2019;18:1534735419835310.
Sekikawa A, Ihara M, Lopez O, Kakuta C, Lopresti B, Higashiyama A, et al. Effect of S-equol and Soy isoflavones on heart and brain. Curr Cardiol Rev. 2019;15(2):114–35.
Shabani P, Izadpanah S, Aghebati-Maleki A, Baghbani E, Baghbanzadeh A, Fotouhi A, et al. Role of miR-142 in the pathogenesis of osteosarcoma and its potential as therapeutic approach. J Cell Biochem. 2019;120(4):4783–93.
Sivonova MK, Kaplan P, Tatarkova Z, Lichardusova L, Dusenka R, Jurecekova J. Androgen receptor and soy isoflavones in prostate cancer. Mol Clin Oncol. 2019;10(2):191–204.
Song M, Tian X, Lu M, Zhang X, Ma K, Lv Z, et al. Genistein exerts growth inhibition on human osteosarcoma MG-63 cells via PPARgamma pathway. Int J Oncol. 2015;46(3):1131–40.
Spagnuolo C, Russo GL, Orhan IE, Habtemariam S, Daglia M, Sureda A, et al. Genistein and cancer: current status, challenges, and future directions. Adv Nutr. 2015;6(4):408–19.
Sun X, Shu Y, Ye G, Wu C, Xu M, Gao R, et al. Histone deacetylase inhibitors inhibit cervical cancer growth through Parkin acetylation-mediated mitophagy. Acta Pharm Sin b. 2022;12(2):838–52.
Varinska L, Gal P, Mojzisova G, Mirossay L, Mojzis J. Soy and breast cancer: focus on angiogenesis. Int J Mol Sci. 2015;16(5):11728–49.
Yang C, Yang QO, Kong QJ, Yuan W, Ou Yang YP. Parthenolide induces reactive oxygen species-mediated autophagic cell death in human osteosarcoma cells. Cell Physiol Biochem. 2016;40(1–2):146–54.
Yang Q, Liu J, Wu B, Wang X, Jiang Y, Zhu D. Role of extracellular vesicles in osteosarcoma. Int J Med Sci. 2022;19(8):1216–26.
Yao J, Wang J, Xu Y, Guo Q, Sun Y, Liu J, et al. CDK9 inhibition blocks the initiation of PINK1-PRKN-mediated mitophagy by regulating the SIRT1-FOXO3-BNIP3 axis and enhances the therapeutic effects involving mitochondrial dysfunction in hepatocellular carcinoma. Autophagy. 2022;18(8):1879–97.
Yin K, Lee J, Liu Z, Kim H, Martin DR, Wu D, et al. Mitophagy protein PINK1 suppresses colon tumor growth by metabolic reprogramming via p53 activation and reducing acetyl-CoA production. Cell Death Differ. 2021;28(8):2421–35.
Yu L, Wei J, Liu P. Attacking the PI3K/Akt/mTOR signaling pathway for targeted therapeutic treatment in human cancer. Semin Cancer Biol. 2022;85:69–94.
Zhang T, Liu Q, Gao W, Sehgal SA, Wu H. The multifaceted regulation of mitophagy by endogenous metabolites. Autophagy. 2022;18(6):1216–39.
Zhang Y, Yin L, Dong J, Xia X. Soy Isoflavones protect neuronal PC12 cells against hypoxic damage through nrf2 activation and suppression of p38 MAPK and AKT-mTOR pathways. Antioxidants (basel). 2022;11(10):2037.
Zhao B, Peng Q, Wang D, Zhou R, Wang R, Zhu Y, et al. Leonurine protects bone mesenchymal stem cells from oxidative stress by activating mitophagy through PI3K/Akt/mTOR pathway. Cells. 2022;11(11):1724.
Zheng G, Wang L, Li X, Niu X, Xu G, Lv P. Rapamycin alleviates cognitive impairment in murine vascular dementia: the enhancement of mitophagy by PI3K/AKT/mTOR axis. Tissue Cell. 2021;69: 101481.
Zhu Y, Yang Z, Xie Y, Yang M, Zhang Y, Deng Z, et al. Investigation of inhibition effect of daidzein on osteosarcoma cells based on experimental validation and systematic pharmacology analysis. PeerJ. 2021;9: e12072.

Publisher's Note